Proceedings of FUELCELL2006
The 4th International Conference on FUEL CELL SCIENCE, ENGINEERING and TECHNOLOGY
June 19-21, 2006, Irvine, CA

FUELCELL2006-97237

TRANSIENT ANALYSIS AND MODELLING OF AUTOMOTIVE PEM FUEL CELL SYSTEM ACCOUNTING FOR WATER TRANSPORT DYNAMICS

Alessandro Miotti
Dipartimento di Elettronica e Informazione
Politecnico di Milano
20133 Milano, Italy
Email: miotti@elet.polimi.it

Alfonso Di Domenico
Dipartimento di Meccanica
Universitá degli Studi di Salerno
84084 Fisciano (SA), Italy
Email: adidomen@unisa.it

Angelo Esposito
Yann G. Guezennec
Center for Automotive Research
The Ohio State University
Columbus, OH, 43212
{esposito.24,guezennec.1}@osu.edu

ABSTRACT

Dynamic behavior and transient analysis are one of the most critical issues for high performance polymeric electrolyte membrane fuel cells. An improvement of performance can be achieved both with hardware modifications and with more sophisticated control strategies. To this regard, the availability of a reliable dynamic fuel cell model plays an important role in the design of fuel cell control and diagnostic system. This paper presents a non-linear, iso-thermal, zero-dimensional model of a pressurized PEM fuel cell system used for automotive applications. The model was derived from a detailed, iso-thermal, steady-state, dimensional model which explicitly calculated (and subsequently captured as a multi-D look-up table) the relationship between cathode and anode pressures and humidity and stack average current. Since in the electrochemical model the single cell performance depends on the membrane ionic resistance, which is strictly related to the membrane water content, a dynamic estimation of the membrane water diffusion has been considered. This takes into account the dependence of the cell voltage on the unsteady membrane water concentration. A similar approach still allows the development of a simple zero-dimensional dynamic model suitable for control system development and amenable to control-oriented humidity modelling.

INTRODUCTION

Due to their high efficiency (about 60% [1], [2]) at normal operating conditions, Proton Exchange Membrane (PEM) fuel cells may represent a valid choice for automotive applications, in the years to come ([3], [4]). The PEM fuel cell includes two electrodes, anode and cathode, separated by a polymeric electrolyte membrane. The ionomeric membrane has exclusive proton permeability and it is thus used to strip electrons from hydrogen atoms on the anode side. The protons flow through the membrane and react with oxygen to generate water on the cathode side and a potential difference between the electrodes [5]. It has been observed that the temperature of the stack needs to be kept around 80^oC for optimal performance (see [6], [5]) and, pressurizing the gases, the fuel cell increases its efficiency and also provides the necessary conditions for smooth fluid flow through the flow channels [7]. The membrane has to be humidified to operate properly, and this is generally achieved through humidification of the air stream [8]. Since the charge transport is related to the water molecules in the membrane, if the electrolyte is partially dehydrated, the ionic resistance increases, hindering the proton flow. On the other hand, the cathode side might be flooded due to an excess of humidification and the gas diffusion layers pores might be occluded, reducing mass transport. Furthermore the anode side experiences an insufficient humidification at high current density, thus enhancing electrolyte ionic conductivity [9]. Since the polymeric membrane regulates and allows mass water transport toward the electrodes, it is one of the most critical fuel cell elements. Particularly, a proper membrane hydration and control are relevant issues to be solved in order to push fuel cell systems toward mass commercialization in automotive applications. Several works proposed in literature focus on the deve-

lopment of detailed dimensional model for water transport phenomena, not suitable for control purposes [10], [11], [12]. The model herein described follows innovative approach to estimate the water transport and concentration dynamics in a zero dimensional structure. This simplified model provides an engineering approximation of the unsteady electro-chemical characteristics of PEM fuel cell stack observed under dynamic load conditions. The computational tool proposed is based on a multi-dimensional map obtained from a dimensional model ([13] and [14]), coupled with a real time estimation of the time constant related to the water diffusion dynamics through the membrane. Consistent with such lumped dynamic model formulation, a filling-emptying approach is followed to model the intake and exhaust manifolds of the gases and the electrodes volumes. In the final part of the paper transient analyses with two different approaches, based on a 1D model [13] and a 1+1D [14] model respectively, are shown.

1 NOMENCLATURE

A_{fc}	Cell active area $[cm^2]$
F	Faraday constant $[\frac{C}{mol}]$
i	Cell current density $[\frac{A}{cm^2}]$
I	Cell current $[A]$
M	Molecular weight $[\frac{kg}{mol}]$
n	Angular speed $[rpm]$
n_e	Number of electrons [-]
N	Number of cells [-]
OCV	Open circuit voltage $[V]$
p	Pressure in the volumes [bar]
R	Gas constant $[\frac{bar \cdot m^3}{kgK}]$
$\bar{\mathrm{R}}$	Universal gas constant $[\frac{bar \cdot m^3}{molK}]$
T	Temperature [K]
V	Volume $[m^3]$
W	Mass flow rate $[\frac{kg}{s}]$
Δp	Pressure difference between the electrodes $[bar]$
λ	Water content [-]
σ	Membrane ionic conductivity $[\frac{\Omega}{cm}]$
ω	Specific humidity [-]
$\tilde{\omega}$	Empirical constant for diffusional overpotential $[\frac{\Omega \cdot cm^2}{K}]$

FOOTERS

an	Anode
ca	Cathode
cp	Compressor
da	Dry air
des	Desired value
dH_2	Dry hydrogen
fc	Fuel cell
H_2	Hydrogen
in	Inlet conditions
lim	Limiting current density
mem	Membrane
N_2	Nitrogen
out	Outlet conditions
O_2	Oxygen
rm	Return manifold
sat	Saturation
sm	Supply manifold
vap	Vapor

2 SYSTEM MODELLING

A proper fuel cell operation may be guaranteed by integrating the fuel cell stack in a structure with an air compressor, humidification chambers, heat exchangers, supply and return manifolds and a cooling system. In order to carry out a model of such a system, solely the main critical dynamics has been considered. Thus, the slowest and fastest dynamics of the system, i.e. the thermal dynamics and electrochemical reactions respectively, has been neglected.

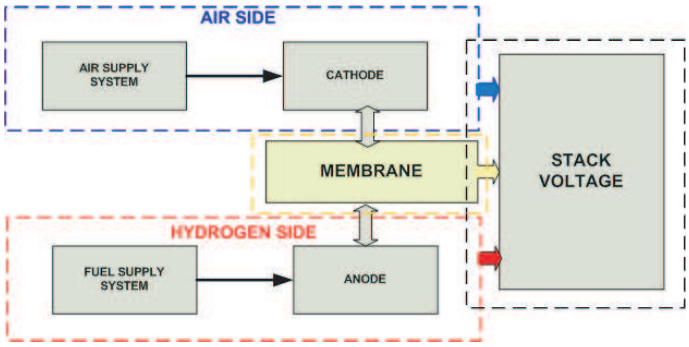

Figure 1. Fuel cell system schematic.

Differential equations representing the dynamics are supported by linear/nonlinear algebraic equations [15].

Consequently, the model presented is substantially based on the following main assumptions: i) spatial variations of variables

are neglected, thus considering a lumped model; ii) all the cells are lumped in one equivalent cell; iii) output flow properties from a volume are equal to the inside properties; iv) fastest dynamics is not considered and is taken into account as static empirical equations; v) all the volumes are isothermal.

An equivalent scheme of the fuel cell system model points out four significant blocks, representing the air supply, the fuel delivery, the membrane behavior and the stack voltage performance (see figure 1).

2.1 Air supply system

The air side includes the compressor, the supply and return manifolds, the cathode volume, the nozzles between manifolds and cathode and the exhaust valve. A screw compressor has been used to pressurize and blow air into the fuel cell stack [16]. The compressor and motor are lumped into a single, second order dynamic system, which is speed driven. The motor-compressor model is separated in two parts. The first part is the second order dynamic system that represents the rotational dynamics associated with the lumped model of compressor and motor. The transfer function representing the dynamics of this subassembly has been identified by means of experimental data and can be approximated by the following:

$$\frac{n_{cp}}{n_{cmd}} = \frac{-3.9610^{-5}s^2 + 0.528s + 567.5}{s^2 + 9.624s + 567.8} \tag{1}$$

where n_{cp} is the speed of the compressor and n_{cmd} is the speed commanded. The second part of the motor compressor assembly model describes the mass flow rate from the compressor via a static map depending on pressure and compressor speed.

For the air side, a supply and a return manifold were represented throughout mass balance and pressure calculation equations [17]. Dry air and vapor pressure in the supply manifold has been described as follows ([15], [18]):

$$\begin{aligned} \frac{dp_{da}}{dt} &= \frac{R_{da}T_{sm,ca}}{V_{sm,ca}}(W_{da,in} - W_{da,out}) \\ \frac{dp_{vap}}{dt} &= \frac{R_{vap}T_{sm,ca}}{V_{sm,ca}}(W_{vap,in} + W_{vap,inj} - W_{vap,out}) \end{aligned} \tag{2}$$

The inlet flows denoted by subscript *in* represent the mass flow rates coming from the compressor. Outlet mass flow rates are determined by using the nonlinear nozzle equation for compressible fluids [19]:

$$W_{out} = \begin{cases} \frac{C_d A_t p_{up}}{\sqrt{RT_{up}}}\left(\frac{p_{dw}}{p_{up}}\right)^{1/\gamma}\sqrt{\frac{2\gamma}{\gamma-1}\left(1-\left(\frac{p_{down}}{p_{up}}\right)\right)^{\frac{\gamma-1}{\gamma}}} \\ \qquad\qquad \text{if} \frac{p_{down}}{p_{up}} > \left(\frac{2}{\gamma+1}\right)^{\frac{\gamma}{\gamma-1}} \\ \frac{C_d A_t p_{up}}{\sqrt{RT_{up}}}\sqrt{\gamma}\left(\frac{2}{\gamma+1}\right)^{\frac{\gamma+1}{2(\gamma-1)}} \\ \qquad\qquad \text{if} \frac{p_{down}}{p_{up}} \leq \left(\frac{2}{\gamma+1}\right)^{\frac{\gamma}{\gamma-1}} \end{cases} \tag{3}$$

where p_{dw} and p_{up} are the downstream and upstream pressure, respectively and R is the gas constant related to the gases crossing the nozzle.

A simplified humidifier has been considered built in the supply manifold. Fixing a desired value of relative humidity for air (ω_{des}), the vapor mass injected (W_{inj}) is obtained through a simplified model accounting for a static mass balance [15]:

$$W_{inj} = W_{da,in}(\omega_{des} - \omega_{in}) \tag{4}$$

where ω is the specific humidity and can be evaluated as follows:

$$\omega_x = \frac{\phi_x \cdot p_{sat}}{p_{da}}\frac{M_{vap}}{M_{da}} \qquad x = des, in \tag{5}$$

In equation (5) ϕ is the relative humidity. Therefore, a first order transfer function has been introduced in order to reproduce the physical behavior of the system. Starting from equations (2), (4) and (5) the supply manifold relative humidity is determined in order to involve the water injection dynamics.

The mass flow rate leaving the supply manifold enters into the cathode volume, where a mass balance for each species (water vapor, oxygen, nitrogen) has been considered [20]:

$$\begin{aligned} \frac{dp_{vap}}{dt} &= \frac{R_{vap}T_{ca}}{V_{ca}}(W_{vap,in} - W_{vap,out} + W_{vap,mem} + \\ &\quad + W_{vap,gen}) \\ \frac{dp_{O_2}}{dt} &= \frac{R_{O_2}T_{ca}}{V_{ca}}(W_{O_2,in} - W_{O_2,out} - W_{O_2,reacted}) \\ \frac{dp_{N_2}}{dt} &= \frac{R_{N_2}T_{ca}}{V_{ca}}(W_{N_2,in} - W_{N_2,out}) \end{aligned} \tag{6}$$

In the equations above, $W_{vap,mem}$ indicates the vapor mass flow rate leaving or approaching the cathode through the membrane, whereas $W_{vap,gen}$ and $W_{O_2,reacted}$ are related to the electrochemical reaction representing the vapor generated and the oxygen reacted, respectively. It has been assumed that all the water generated passes in the vapor form. In Equation (6), p is the partial

pressure of each element and thus the cathode pressure is given by Dalton law:

$$p_{ca} = p_{vap} + p_{O_2} + p_{N_2} \tag{7}$$

The gases leaving the cathode volume are collected inside the return manifold which has been modelled using an overall mass balance for the moist air:

$$\frac{dp_{rm,ca}}{dt} = \frac{R_{da}T_{rm,ca}}{V_{rm,ca}}(W_{air,in} - W_{air,out}) \tag{8}$$

In order to control the pressure in the air side volumes, an exhaust valve has been applied following the same approach of equation (3) where the cross sectional area may be varied accordingly to a control command.

2.2 Fuel Side

As seen for the air side, three volumes have been taken into account: supply and return manifolds and anode. A humidification model similar to the cathode side has been applied. Equations (2), (4) and (5) have been particularized for the hydrogen side, leading to the following balance for the fuel supply manifold [21]:

$$\begin{aligned} \frac{dp_{dH_2}}{dt} &= \frac{R_{dH_2}T_{sm,an}}{V_{sm,an}}(W_{dH_2,in} - W_{dH_2,out}) \\ \frac{dp_{vap}}{dt} &= \frac{R_{vap}T_{sm,an}}{V_{sm,an}}(W_{vap,in} + W_{vap,inj} - W_{vap,out}) \end{aligned} \tag{9}$$

where $W_{H_2,in}$ is the hydrogen inlet flow supplied by a fuel tank which is assumed to have an infinitive capacity and an ideal control capable to satisfy the required current density. Especially, the delivered fuel depends on the stoichiometric hydrogen and it is related to the utilization coefficient in the anode (u_{H_2}):

$$W_{H_2,in} = A_{fc}N\frac{i \cdot M_{H_2}}{n_e F}u_{H_2} \tag{10}$$

In the equation above, A_{fc} and N are the fuel cell active area and the number of cells in the stack; u_{H_2} is kept constant and indicates the amount of reacted hydrogen. Regarding the outlet flow from the supply manifold, $W_{H_2,out}$, it has been determined through the nozzle equation (3). As previously done for the cathode, mass balance equation has been implemented for the anode:

$$\begin{aligned} \frac{dp_{vap}}{dt} &= \frac{R_{vap}T_{an}}{V_{an}}(W_{vap,in} - W_{vap,mem} - W_{vap,out}) \\ \frac{dp_{H_2}}{dt} &= \frac{R_{H_2}T_{an}}{V_{an}}(W_{H_2,in} - W_{H_2,out} - W_{H_2,reacted}) \end{aligned} \tag{11}$$

where $W_{vap,in}$ is the inlet vapor flow set to zero as assumed before, $W_{vap,mem}$ is the vapor flow crossing the membrane and $W_{vap,out}$ represents the vapor flow collecting in the return manifold through the nozzle (eq. 3). Referring to the return manifold, the same approach of equation (8) has been followed.

3 MEMBRANE

The gas and water properties are influenced by the relative position along both the electrodes and the membrane thickness. Consequently, a suited treatment should be represented by partial differential equations. However, a fast computational time is a significant issue and considering the difficulties related to the parameters identification for the membrane mass transport and the electrochemical phenomena, static maps are preferred to the physical model.

Nevertheless, in order to preserve the accuracy of a dimensional approach, two static maps have been carried out using a one dimensional model and a 1+1D model respectively.

The one dimensional model describes system properties as a function of membrane thickness, while the 1+1D model accounts for properties spatial variations along the electrodes length, integrating the previous 1D model as a map. The reader is addressed to previous works ([13] and [14]) for further details, omitted in this paper for brevity.

3.1 Model based on one dimensional model

As mentioned above, the 1D model accounts just for the spatial variation along the membrane thickness, neglecting the properties profile related to the electrodes dimension. The inputs for this model are represented by the mean values of electrodes water content (λ_{ca}, λ_{an}), pressure difference at the electrodes (Δ_p) and the current density (i). Based on these inputs, a dimensional map has been built, giving as outputs the net water flux across the membrane and the profile of water content along the electrolyte. As well known, a zero dimensional model requires a mean value for each property, so that the lumped water concentration has been computed as follows:

$$\overline{\lambda_{1D}} = \frac{1}{N_{mem}}\sum_{i=1}^{n}\lambda_i \tag{12}$$

where λ_i is the value of water content for each slice of the membrane. In order to imbed the map in the zero dimensional model, the electrodes properties have been defined accordingly to equation (6), (11) and to the empirical equation [13]:

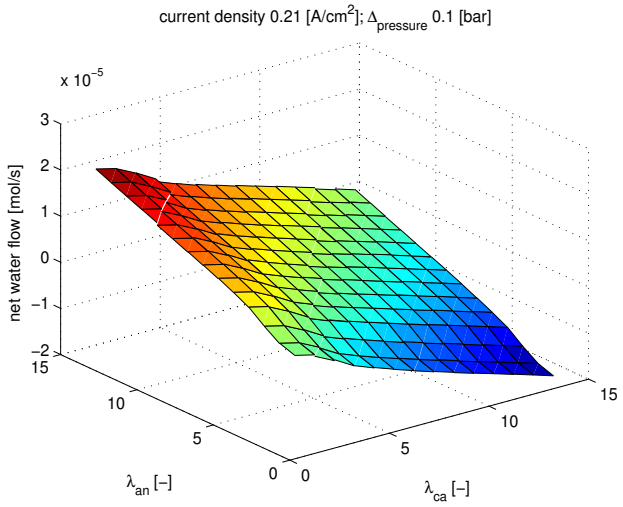

Figure 2. Membrane water flux as a function of λ at both the electrodes.

$$\lambda_x = \begin{cases} 0.3 + 10.8\phi_x - 16.0\phi_x^2 + 14.1\phi_x^3 & \text{if} \quad 0 \leq \phi_x < 1 \\ -30.41 + 61.98\phi_x - 25.96\phi_x^2 + 3.70\phi_x^3 & \text{if} \quad \phi_x \geq 1 \end{cases} \tag{13}$$

where x refers either to the anode or to the cathode.

Figure 2 shows the membrane water flow behavior as a function of λ at both the electrodes, fixing cathode pressure and current density. This approach allows to obtain the map easily and with short computational time, without changing radically the basic structure of a filling-emptying model. However, a different approach may be followed in order to take into account the properties profile along the electrodes.

3.2 Model based on 1+1 D model

The 1+1D model describes system properties as a function of the electrodes length, accounting for an integrated one dimensional map, derived from the 1D model previously described (see figure 3). Explicitly, the imbedded map for the membrane is solved for each slice of the electrodes length, providing the net water flux (N_w) and the concentration value needed to evaluate the electrode property profiles.

The most critical variables affecting system operation and its performance have been taken into account as inputs for a multi-dimensional map:

current density;
cathode pressure;
anode pressure;
cathode inlet humidity.

A complete operating range of the variables above has been supplied to the 1+1-dimensional model, in order to investigate the electrolyte and cell operating conditions and to obtain the corresponding water flow starting from each set of inputs.

Thus, the membrane map outputs the net water flow crossing the membrane (calculated as $\sum N_w$) and it points out water content ($\overline{\lambda_{1+1D}} = \frac{1}{N_el}\sum_{i=1}^{n}\lambda_i$) during cell operation. Figure 4 shows the membrane water flow behavior as a function of the current density and the pressure difference between the electrodes, fixing anode and cathode pressure and relative humidity.

The second approach is more accurate than the previous one, as the map has been derived from a quasi 2D model. Nevertheless, map building requires long off-line computational time, it is more sensitive and leads to modify the filling-emptying structure of the electrodes.

4 MEMBRANE DYNAMICS

An arduous task in fuel cell modelling is to relate its performance to the gases humidity and membrane water content. Since the resistance to proton transfer through the membrane is strictly dependent on membrane water content, the water transport phenomena have to be considered to describe fuel cell performance and dynamics. Water migrates inside the membrane because of electro-osmotic drag, pressure-driven convective transport and diffusive transport [8]. The right approach to describe water transport is to consider an equation that takes in account all those mechanisms, but for control-model purpose phenomena time-constants are more important. It has seen that the time-constant related to pressure-driven transport is negligible because of the difference of pressure between cathode and anode is very small (0.1 bar). Also, it is reasonable to assume the same dynamics both for electro-osmotic drag and diffusive transport, since the electro-osmotic coefficient (n_d) and the effective diffusion coefficient (D_w^{eff}) are estimated with a similar function of the membrane water content [17]. So the dynamics of net water transport can be just evaluated through the water diffusion one.

Particularly, the diffusion coefficient is expressed as follows [11]:

$$D_w^{eff} = (d_1 + d_2\lambda + d_3\lambda^2 + d_4\lambda^3) \cdot exp(d_5(\frac{1}{d_6} - \frac{1}{T_{fc}})) \tag{14}$$

where d_1,d_2,d_3,d_4 and d_5 are empirical constants [12]. Diffusion transport is here described with unsteady 1D equation, assuming diffusion normal to the face of the electrodes as main mechanism [22]:

$$\frac{\partial \Gamma}{\partial t} = D_w^{eff}\frac{\partial^2 \Gamma}{\partial z^2} \tag{15}$$

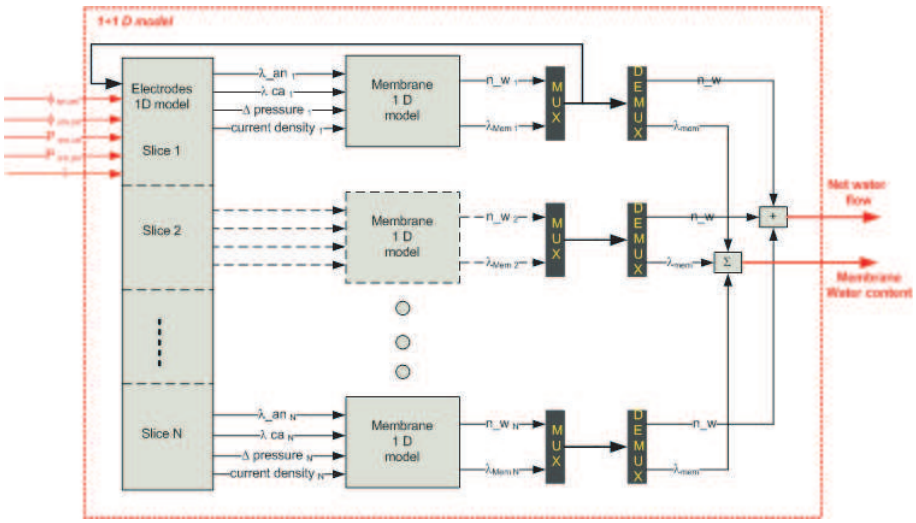

Figure 3. Schematic representation of the 1+1D model, integrating the map derived from the 1D model.

where Γ is the dimensionless water concentration. It has been hypothesized that the concentration variation occurs only at one side. Thus, a well-known good approximate solution of equation (15) is [22]:

$$\Gamma = 1 - erf(\eta) \tag{16}$$

where η is a combination of the space (z) and time (t) variables:

$$\eta = \frac{z}{\sqrt{4 \cdot D_w^{eff} t}} \tag{17}$$

and erf is the error function, describing the development of the water concentration profile. It is possible to model water concentration evolution choosing proper values for η and fixing z equal to the membrane thickness. Particularly, a time-delay can be find out reshaping equation (17) and assuming η=2.34, so that Γ is equal to 0.01, which translates in a membrane water concentration of 1% of the regime value. A time-constant for water content variation can be estimated choosing η=0.0443, leading to a value of Γ equal to 0.95. The latter value includes the time-delay as well. It is worth noting that D_w^{eff} is not a constant, but varies accordingly with water content, leading to an appropriate time-varying time constant. In such a way the water transport dynamics is slow if the water content is low and speeds up when water content increases, as shown in Figure 5.

Ultimately, starting from a steady-state value of water content a first order dynamics, based on the mentioned time constant,

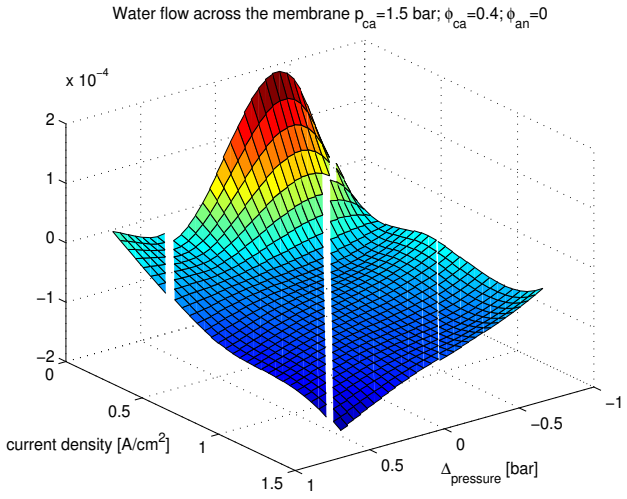

Figure 4. Membrane water flux as a function of current density and pressure difference at constant anode and cathode pressure and relative humidity.

is introduced. The steady-state value of water content is estimated with both the map from the 1D model and the map from the 1+1D model.

5 STACK VOLTAGE MODEL

As long as hydrogen and oxygen are fed to the fuel cell stack, electrochemical reactions take place generating a potential difference at the electrodes. When the load is not connected

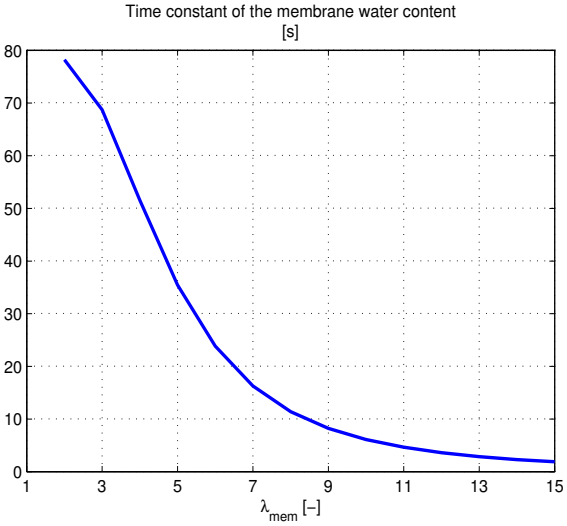

Figure 5. Water content time constant as a function of λ.

to the cell, the open circuit voltage may be defined as a function of pressure and temperature of the reactants [9]:

$$OCV = 1.23 - 0.9 \cdot 10^{-3}(T_{fc} - 298) + \frac{\bar{\mathrm{R}}T}{4F} ln(p_{H_2}^2 \cdot p_{O_2}) \quad (18)$$

Unlikely, cell ideal voltage is not achievable under operating conditions due to several cell irreversible processes which occur when a load is applied to the stack. Consequently, the cell voltage drops as the current increases due to the losses phenomena mainly related to activation, diffusional and ohmic and polarizations.

The activation overpotential is the result of the effective electron transfer and of the chemical bonds breaking and forming at the cathode and anode. The required energy for the process is supplied by the fuel used in the fuel cell, reducing the available energy to produce electric power. The activation losses can be defined as follows [9]:

$$V_{act} = \frac{\bar{\mathrm{R}}T}{F} ln \frac{i}{i_0} \quad (19)$$

The diffusional polarization is due to the resistance to the mass transport of gases to reactions sites and to the removal of impurities and generated water. Consequently, the efficiency of the reactions sites is reduced because the concentration of the provided reactants is lower than the ideal quantity. The diffusional polarization has been modelled as follows [9]:

$$V_{diff} = \widetilde{\omega} T_{fc} i \cdot ln(\frac{i_{lim}}{i_{lim} - i}) \quad (20)$$

where $\widetilde{\omega}$ id an empirical constant for diffusional overpotential [9] and i_{lim} is the limiting current density, that is the current density for which the voltage drops to zero.

The ohmic polarization is related to the electrical cell resistance. Thus, the ohmic overpotential has been implemented as [9]:

$$V_{ohm} = r \cdot i \quad (21)$$

The cell resistance depends on the membrane ionic conductivity expressed as a function of the membrane water content [11]:

$$\sigma_{mem} = a_1 \cdot \lambda_{mem} - a_2 \cdot \lambda_{mem} \cdot \exp(a_3 \cdot (\frac{1}{303} - \frac{1}{T_{fc}})) \quad (22)$$

where a_1, a_2 and a_3 are empirical constants found in literature [11]. Afterwards, the cell resistance is given by the rate between the membrane thickness and the membrane ionic conductivity [11]. Starting from the mentioned potential losses, the output cell voltage can be estimated by the following relationship [9]:

$$V_{fc} = OCV - V_{act} - V_{diff} - V_{ohm} \quad (23)$$

Throughout equation (23), the polarization curve of the cell has been derived. The paper focuses on the characterization of the dependance of the cell voltage behavior on the membrane water content (λ). Several values of the membrane water concentration lead to different voltage response, as shown in figure 6.

One of the most relevant issues for proper cell operation is to keep the membrane humidification above a certain value in order to guarantee enough ionic conductivity. Indeed, low water concentration is revealed by poor cell performance (see Figure 6).

Due to the close relationship between voltage and λ, it is clear that, in order to satisfy the fast dynamic response required from automotive applications, the water concentration dynamic behavior plays a significant role influencing the cell voltage performance.

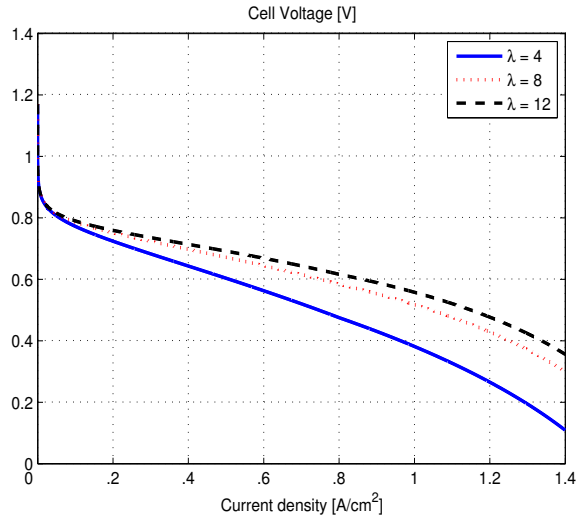

Figure 6. Polarization curves for different values of λ.

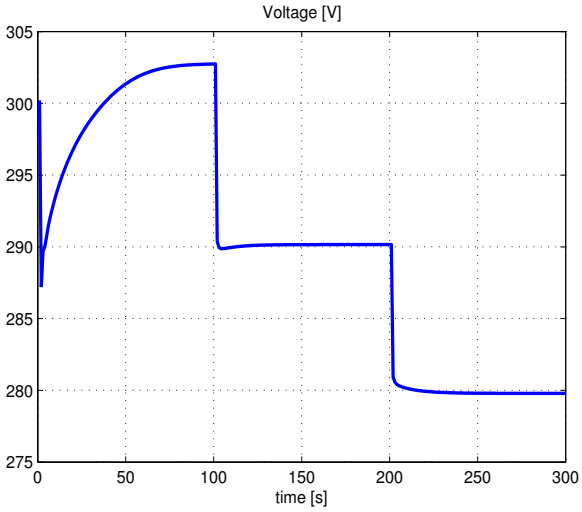

Figure 7. Voltage behavior due to three steps of current, increasing membrane water concentration.

The figure 7 represents the voltage profile due to three different steps of current, while the water concentration in the membrane is increasing. The first step of current occurs at a very poor membrane humidification, resulting in a very slow dynamic voltage response. However, as the water content reaches proper values, the dynamic response becomes significantly faster.

6 FEED-FORWARD CONTROL

Since the fuel cell system has to satisfy all the current demand, the stack must not suffer for oxygen starvation. In fact, the air mass flow rate decreases for each load change and the control system has to avoid every fast cell starvation during the transient, while following the optimal pressure [23], [24].

Furthermore, the current demand translates into a requested air mass flow rate, determined fixing the air excess ratio to a value equal to 2 [24]. The feed forward control is the simplest way to assure a proper fuel cell system operation, obtaining a fast and quite sharp control on the system performance. In order to analyze and investigate the model described through simulations, a feed forward control is required. Applying three different static maps, the actuators of the system, namely the compressor, the air and fuel side back-pressure valves, may be properly tuned.

7 RESULTS

The model and the corresponding simulator, developed in Matlab/Simulink, is based on the parameters and geometrical data [25] of a $60kW$ fuel cell system, shown in table 1.

Variable	Values
Active cell area $[cm^2]$	312
Membrane thickness $[\mu m]$	51
Number of cells $[-]$	385
Desired cathode relative humidity $[-]$	0.6
Inlet anode relative humidity $[-]$	0
Max current demand $[A]$	230
Fuel cell temperature $[K]$	353
Fuel utilization $[-]$	0.9
Excess of air $[-]$	2

Table 1. Fuel cell parameters

To appreciate the dynamic behavior of the system, a series of steps in current has been introduced and implemented as the requested load (see figure 8).

7.1 Results of the 1D model

In this section, the results of the simulations performed, imbedding the map derived by the 1D model, are presented. Figure 9 shows the different effects of the water concentration on the voltage response.

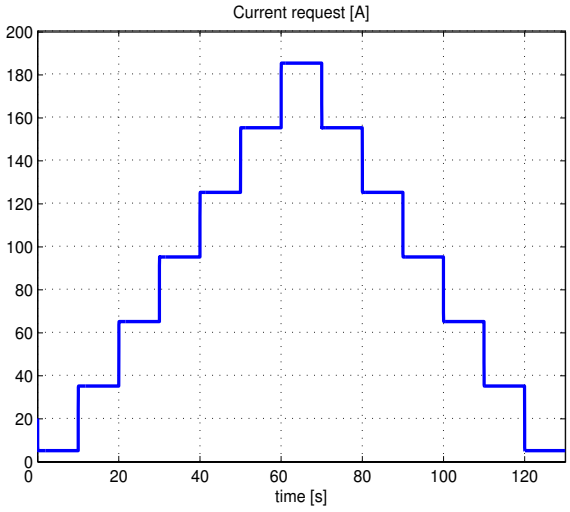

Figure 8. Series of steps in current.

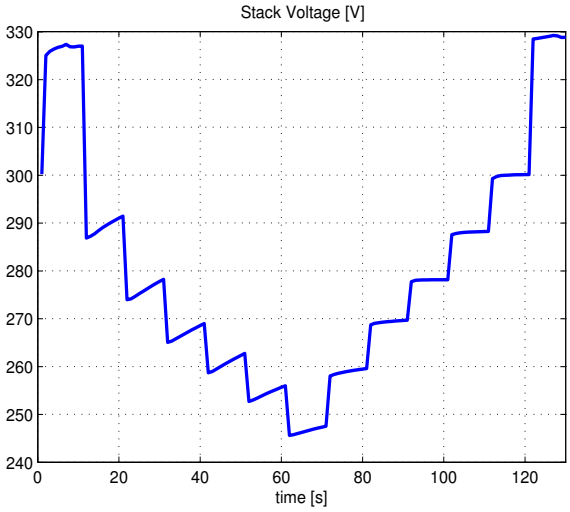

Figure 9. Voltage response for a series of current.

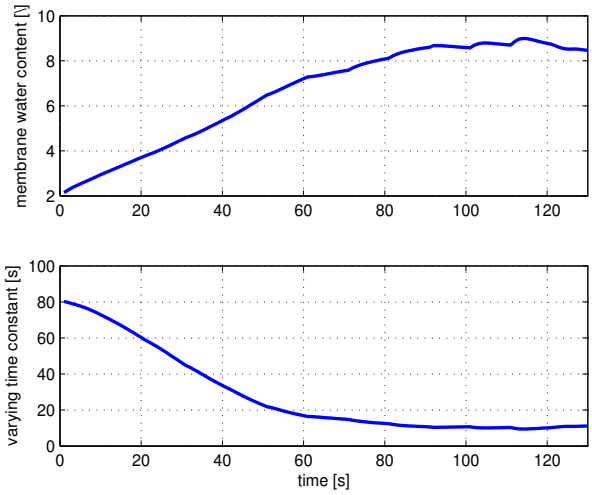

Figure 10. Membrane water content.

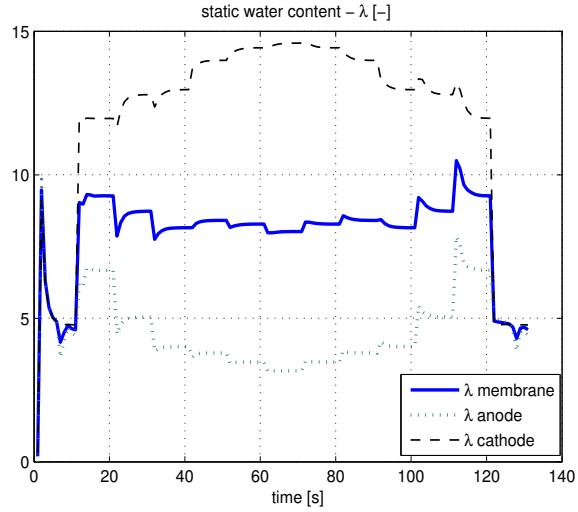

Figure 11. Membrane static water content calculated by the 1D map, compared with the λ at the electrodes.

At the starting point the membrane is almost totally dehydrated leading to a slow voltage transient. However, as the current increases, the membrane water content increases as well, resulting in improved cell performance and faster response to load changes. Thus, it may be stated that the dynamics related to the membrane water concentration is one of the slowest to take into account for fuel cell system design and control.

Figure 10 depicts what mentioned above, showing the membrane humidification dynamics for the provided current steps and related time constant, defined through the approach presented by equations (15, 16 and 17).

The trend of λ, shown in figure 10, is obtained applying a first order dynamic with the varying time constant τ to the static values provided by the imbedded map. Figure 11 illustrates the static membrane water content, compared with the water concentration for both the electrodes.

In this case, the anode and cathode water content has been derived by equation (13), based on the relative humidity calculated through the filling emptying methodology. On the other hand, this approach neglects the relative humidity profile as a function of the electrodes length.

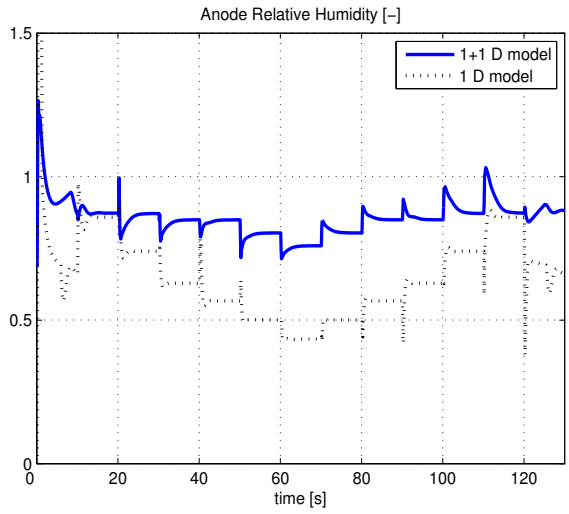

Figure 12. Comparison of the anode relative humidity due to current steps for the two proposed model.

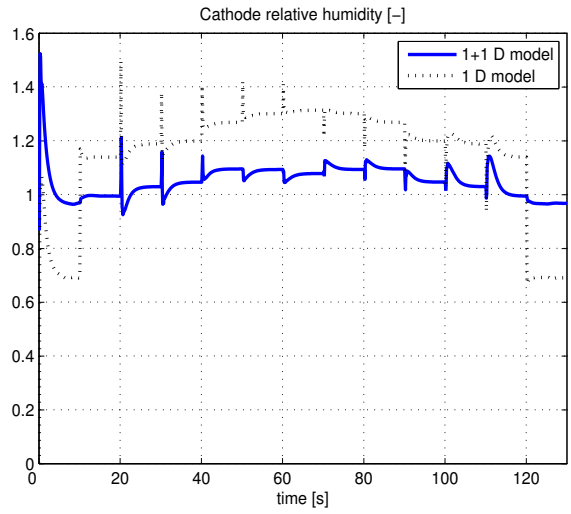

Figure 13. Comparison of the cathode relative humidity due to current steps for the two proposed model.

7.2 Comparison between 1D and 1+1D model

The second approach proposed allows to take into account the dependency of the anode and cathode humidity along the electrodes length. For this reason, the model presented leads to more realistic results than the previous one, especially in the estimation of the relative humidity of the electrodes. Figures 12 and 13 highlight a comparison between the two model proposed in the evaluation of the relative humidity in the anode and cathode respectively.

As clear, in figure 12 and 13, the approach based on the 1D model underestimates the anode humidity while overestimates the cathode one. In fact one of the assumption of the filling-emptying method states that the output property values are equal to the inner ones. However, as it can be seen in figure 14, the output humidity at the cathode side is higher than the value provided by the control volumes approach. This results in an underestimation of the vapor flow rate leaving the cathode, thus computing an higher value for the inner humidity. In the same way, the relative humidity for the anode side is underestimated.

Even if a more realistic result has been achieved imbedding 1+1D model, the voltage performance and the membrane water content do not improve in a significant way. Figures 16 and 15 show a comparison between the two models in the evaluation of the net water flow crossing the membrane and cell voltage.

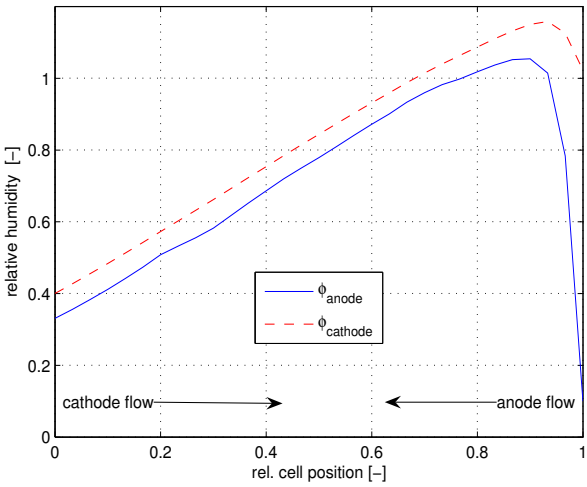

Figure 14. Anode and cathode relative humidity as a function of the electrolyte thickness for a counter flow structure [14].

8 CONCLUSION AND FUTURE WORKS

A simulation model for Proton Exchange Membrane fuel cell for automotive system has been developed. Two different approaches have been followed and investigated in order to perform the voltage and membrane water content behavior. The model herein described includes an innovative approach for the evaluation of the electrolyte water concentration dynamics for a zero dimensional model. Preserving the accuracy of the dimensional model, the simulation tool proposed experiences a fast computational time. In conclusion, the developed model is a starting point for analysis and control of a fuel cell system for ground transportation.

A number of extension of this work are currently underway.

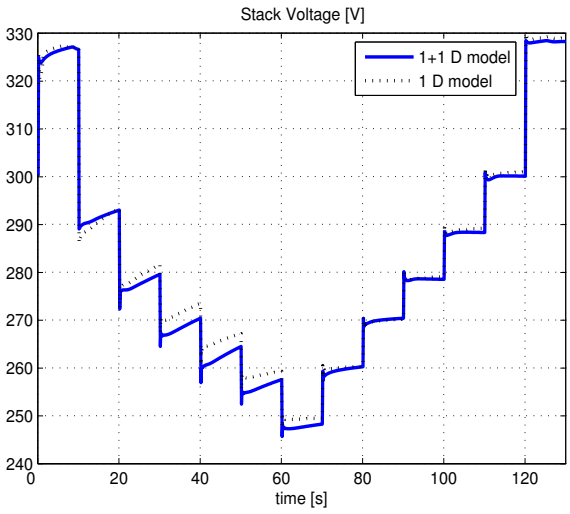

Figure 15. Comparison of the voltage responses for the two different approaches.

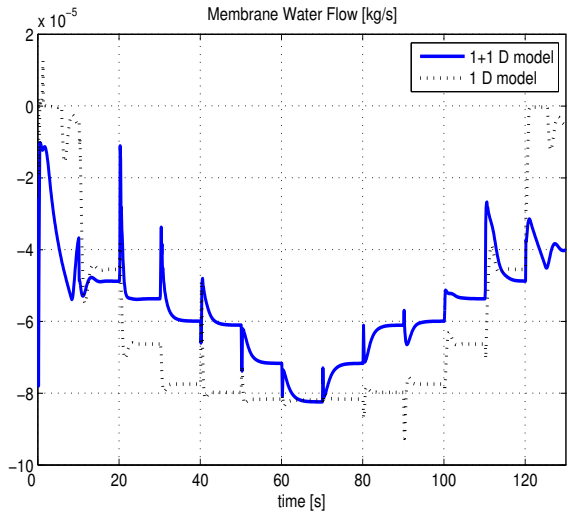

Figure 16. Comparison of the membrane water content for the two different approaches.

Especially, the most important future improvement to the model will consider that the water generated by the reaction is in liquid form and do not evaporate instantaneously. Consequently, two different mass balances will be considered both for the liquid water and for the vapor.

ACKNOWLEDGMENT

Fruitful discussions with Nadia Anguiano are gratefully acknowledged. The Doctoral fellowship of Alfonso Di Domenico is granted by European Union.

REFERENCES

[1] Brinkman, N., 2002. "Well to wheel energy use and greenhouse gas emission of advanced fuel/vehicle system - north american analysis". *General Motors Executive Summary Report, available at the http://www.epa.gov*, pp. 139–152.

[2] Davis, C., Edelstein, B., Evenson, B., and Brecher, A., 2003. "Hydrogen fuel cell vehicle study". *American Physical Society Report available at the http://www.aps.org*.

[3] Thijssen, J., and Teagan, W., 2002. "Long-term prospects for pemfc and sofc in vehicle applications". *SAE paper 2002-01-0414*.

[4] Bernay, C., Marchanda, M., and Cassir, M., 2002. "Prospects of different fuel cell technologies for vehicle applications". *Journal of Power Sources 108*, pp. 139–152.

[5] Larminie, J., and Dicks, A., 2003. *Fuel Cell System Explained*. Wiley.

[6] U.S. DEPARTMENT OF ENERGY - NATIONAL ENERGY TECHNOLOGY LABORATORY STRATEGIC CENTER FOR NATURAL GAS, 2002. *Fuel Cell Handbook - Sixth edition*.

[7] Yi, J., Yang, J. D., and King, C., 2004. "Water management along the flow channels of pem fuel cells". *AIChE Journal*.

[8] Chen, D., and Peng, H., 2004. "Modeling and simualtion of a pem fuel cell humidification system". *Proceeding of the 2004 American Control Conference*.

[9] Maggio, G., Recupero, V., and Pino, L., 2001. "Modeling polymer electrolyte fuel cells: an innovative approach". *Journal of Power Sources 101*, pp. 275–286.

[10] Djilali, N., and Lu, D., 2002. "Influence of heat transfer of gas and water transport in fuel cell". *International Journal of Thermal Science , pp. 29-40*.

[11] Springer, T. E., Zawodzinski, T. A., and Gottesfeld, S., 1993. "Polymer electrolyte fuel cell model". *Journal of the Electrochemical Society 138(8)*, pp. 2334–2341.

[12] Costamagna, P., 2001. "Transport phenomena in polymeric membrane fuel cells". *Chemical Engineering Science, pp. 323-332*.

[13] Mazunder, S., 2003. "A generalized phenomenological model and database for the transport of water and current in polymer electrolyte membranes". *Journal of Electrochemical Society*.

[14] Ambuhl, D., Anguiano, N., Sorrentino, M., Y. Guezennec, S. M., and Rizzoni, G., 2005. "1&1d isothermal steady state model of a single pem fuel cell". In Proceedings of 2005 IMECE, Orlando, FL, U.S.A.

[15] Kueh, T., Ramsey, J., and Threlkeld, J., 1998. *Thermal Enviromental Engineering*. McGraw Hill.

[16] Guzzella, L., 1999. "Control oriented modeling of fuel cell based vehicles". *NSF Workshop on the Integration of Modeling and Control for Automotive System*.

[17] Pukrushpan, J., 2003. "Modeling and control of fuel cell system and fuel processor". PhD thesis, The University of Michigan, Ann Arbor, U.S.A.

[18] Pukrushpan, J., Stefanopulou, A., and Peng, H., 2002. "Modeling and control for pem fuel cell stack system". *Proceeding of American Control Conference*, pp. 3117–3122. Anchorage,AK.

[19] Heywood, J., 1998. *Internal Combustion Engine Fundamentals*. McGraw Hill.

[20] Pukrushpan, J., Stefanopulou, A., and Peng, H., 2004. "Simulation and analysis of transient fuel cell system performance based on dynamic reactant flow model". In Proceedings of 2002 ASME International Mechanical Engineering Conference and Exposition.

[21] Arsie, I., Di-Domenico, A., Pianese, C., and M.Sorrentino, 2005. "Transient analysis of pem fuel cell for hybrid vehicle application". *Proceedings of 2005 ASME 3rd Int. Conference on Fuel Cell Science, Ypsilanti, MI*.

[22] Bird, R., Stewart, W., and Lightfoot, E., 2002. *Transport Phenomena*. John Wiley and Sons.

[23] Bansal, D., Rajagopalan, S., Choi, T., Guezennec, Y., and Yurkovich, S., 2004. "Pressure and air fuel ratio control of pem fuel cell system for automotive traction". *IEEE - VPP conference*.

[24] Di-Domenico, A., Miotti, A., and S.V. Rajagopalan, Y. G., 2005. "Control-oriented model for an automotive pem fuel cell system with imbedded 1+1d membrane water transport". *IEEE Vehicle Power and Propulsion Conference*.

[25] Rodatz, P., 2003. "Dynamics of the polymer electrolyte fuel cell: Experiments and model-based analysis". PhD thesis, Swiss federal Institute of technology, Zurich, Swiss.